

Dalton Transactions

Accepted Manuscript



This is an *Accepted Manuscript*, which has been through the Royal Society of Chemistry peer review process and has been accepted for publication.

Accepted Manuscripts are published online shortly after acceptance, before technical editing, formatting and proof reading. Using this free service, authors can make their results available to the community, in citable form, before we publish the edited article. We will replace this *Accepted Manuscript* with the edited and formatted *Advance Article* as soon as it is available.

You can find more information about *Accepted Manuscripts* in the [Information for Authors](#).

Please note that technical editing may introduce minor changes to the text and/or graphics, which may alter content. The journal's standard [Terms & Conditions](#) and the [Ethical guidelines](#) still apply. In no event shall the Royal Society of Chemistry be held responsible for any errors or omissions in this *Accepted Manuscript* or any consequences arising from the use of any information it contains.

Syntheses, Crystal Structures, UV-Visible Absorption Properties of Five Metal-Organic Frameworks Constructed From Terphenyl-2,5,2',5'-tetracarboxylic Acid and Bis(imidazole) Bridging Ligands

Liming Fan,^{a,b} Xiutang Zhang,^{*a,b} Wei Zhang,^b Yuanshuai Ding,^b Weiliu Fan,^a Liming Sun,^a Yue Pang,^a Xian Zhao^{*a}

Received (in XXX, XXX) Xth XXXXXXXXXX 2014, Accepted Xth XXXXXXXXXX 2014

First published on the web Xth XXXXXXXXXX 2014

DOI: 10.1039/c3dt00000x

ABSTRACT: Solvothermal reactions of terphenyl-2,5,2',5'-tetracarboxylic acid (H_4tptc) and transition metal cations (Ni^{II} , Mn^{II}) afford five novel coordination polymers (CPs) in the presence of four bis(imidazole) bridging ligands (1,3-bimb = 1,3-bis(imidazol-1-ylmethyl)benzene, 1,4-bmib = 1,4-bis(2-methylimidazol-1-ylmethyl)benzene, 4,4'-bibp = 4,4'-bis(imidazol-1-yl)biphenyl, 4,4'-bimbp = 4,4'-bis(imidazol-1-ylmethyl)biphenyl), namely, $[M(tptc)_{0.5}(1,3-bimb)(H_2O)]_n$ ($M = Ni$ for **1**, Mn for **2**), $\{[Ni(tptc)_{0.5}(1,4-bmib)] \cdot 0.25H_2O\}_n$ (**3**), $\{[Ni(tptc)_{0.5}(4,4'-bibp)_2(H_2O)] \cdot 2H_2O\}_n$ (**4**), and $\{[Ni(tptc)_{0.5}(4,4'-bimbp)_{1.5}(H_2O)] \cdot H_2O\}_n$ (**5**). Their structures have been determined by single-crystal X-ray diffraction analyses and further characterized by elemental analyses, IR spectra, powder X-ray diffraction (PXRD), and thermogravimetric (TG) analyses. Complexes **1** and **2** are isomorphous and exhibit a 3D (3,4)-connected **tfi** framework with the Point Schläfli symbol of $(4 \cdot 6^2)(4 \cdot 6^6 \cdot 8^3)$. Complex **3** shows an unprecedented 3D (4,4)-connected framework with the Point Schläfli symbol of $(4 \cdot 6^4 \cdot 8^2)_2(4^2 \cdot 8^4)$. Complex **4** displays a novel 2D self-catenating 5-connected network with the Schläfli symbol of $(4^6 \cdot 6^4)$ based on three interpenetrating 4^4 -**sql** subnets. Complex **5** features a 2D 3-connected 6^3 -**hcb** network built from interesting chains with loops. To the best of our knowledge, the 3D (4,4)-connected $(4 \cdot 6^4 \cdot 8^2)_2(4^2 \cdot 8^4)$ host-framework of **3** and 2D self-catenating 5-connected $(4^6 \cdot 6^4)$ network of **4** have never been documented to date. Moreover, the UV-Visible absorption spectra of complexes **1–5** have been investigated.

Introduction

The design and synthesis of coordination polymers (CPs) have attracted upsurging research interest not only because of their appealing structural and topological novelty but also owing to their tremendous potential applications as functional materials such as in gas storage, microelectronics, chemical separations, nonlinear optics, drug delivery, molecular magnetism, and heterogeneous catalysis.^{1–3} Generally speaking, the structural diversity of such crystalline materials dependent on many factors, such as metal ion, templating agents, metal-ligand ratio, pH value, counteranion, and number of coordination sites provided by organic ligands.^{4,5} Among the strategies, the rational selection of organic ligands or coligands according to their length, rigidity, and functional groups is important for the assembly of structural controllable CPs, and a great deal of significant works have been done by using the strategy.⁶ Usually, the organic ligands with bent backbones, such as V-shaped, triangular, quadrangular, and

so on, are excellent candidates for building highly high-connected, interpenetrating, or helical coordination frameworks due to their bent backbones and versatile bridging fashions.^{7,8} Besides, the carboxylate groups are good hydrogen-bond acceptor as well as donor, depending upon the degree of deprotonation. Among which, quadrangular polycarboxylic acids, such as 1,3,4,5-benzenetetracarboxylic acid, 3,3',5,5'-biphenyltetracarboxylic acid, 2,2',5,5'-biphenyltetracarboxylic acid, 2,2',4,4'-biphenyltetracarboxylic acid, 3,3',5,5'-terphenyltetracarboxylic acid, are paid much attention due to their rich coordination modes.⁹ Apart from the carboxylate linkers, bis(imidazole) bridging ligands with different length and flexibly, such as 1,3-bis(1-imidazolyl)benzene, 1,4-bis(1-imidazolyl)benzene, 1,4-bis((1-imidazolyl)-2,5-dimethylbenzene), 1,3-bis(imidazol-1-ylmethyl)benzene, 1,4-bis(imidazol-1-ylmethyl)benzene, 1,4-bis(2-methylimidazol-1-ylmethyl)benzene, 4,4'-bis(imidazol-1-yl)biphenyl, 4,4'-bis(imidazol-1-ylmethyl)biphenyl, 2,7-bis(1-imidazolyl)fluorene are frequently used in the assembly process of CPs as bridging linkers, guest molecules, or charge balance roles.¹⁰

Thus, these considerations inspired us to explore new coordination architectures with terphenyl-2,5,2',5'-tetracarboxylic acid (H_4tptc) and four (bis)imidazole bridging linkers (1,3-bimb, 1,4-bmib, 4,4'-bibp, and 4,4'-bimbp). In this paper, we reported the syntheses and characterizations of

^a State Key Laboratory of Crystal Materials, Shandong University, Jinan 250100, China. E-mail: zhaoxian@icm.sdu.edu.cn.

^b Advanced Material Institute of Research, College of Chemistry and Chemical Engineering, Qilu Normal University, Jinan, 250013, China. E-mail: xiutangzhang@163.com.

† Electronic Supplementary Information (ESI) available: Additional Figures, IR spectra, Powder XRD patterns and X-ray crystallographic data, CCDC 973827-973831 for 1-5. See DOI:10.1039/c3dt00000x.

five novel CPs, namely, $[\text{M}(\text{tptc})_{0.5}(\text{1,3-bimb})(\text{H}_2\text{O})_n]_n$ ($\text{M} = \text{Ni}$ for **1**, Mn for **2**), $\{[\text{Ni}(\text{tptc})_{0.5}(\text{1,4-bmib})] \cdot 0.25\text{H}_2\text{O}\}_n$ (**3**), $\{[\text{Ni}(\text{tptc})_{0.5}(\text{4,4'-bibp})_2(\text{H}_2\text{O})] \cdot 2\text{H}_2\text{O}\}_n$ (**4**), and $\{[\text{Ni}(\text{tptc})_{0.5}(\text{4,4'-bimbp})_{1.5}(\text{H}_2\text{O})] \cdot \text{H}_2\text{O}\}_n$ (**5**), which exhibit a systematic variation of architectures from 2D layers to 3D frameworks.

Experimental Section

Materials and Physical Measurements. All chemicals were purchased from Jinan Henghua Sci. & Tec. Co. Ltd. without further purification. IR spectra were measured on a Nicolet 740 FTIR Spectrometer at the range of 600–4000 cm^{-1} . Elemental analyses were carried out on a CE instruments EA 1110 elemental analyzer. X-ray powder diffractions were measured on a Panalytical X-Pert pro diffractometer with $\text{Cu-K}\alpha$ radiation. Thermogravimetric analyses were performed under air condition from room temperature to 800 $^\circ\text{C}$ with a heating rate of 10 $^\circ\text{C min}^{-1}$ on Perkin-Elmer TGA-7 thermogravimetric analyzer. Solid UV–visible spectra were obtained in the 200–800 nm range on a JASCOVIDEC-660 spectrophotometer.

Synthesis of $[\text{Ni}(\text{tptc})_{0.5}(\text{1,3-bimb})(\text{H}_2\text{O})_n]_n$ (1**).** A mixture of H_4tptc (0.15 mmol, 0.050 g), 1,3-bimb (0.20 mmol, 0.048 g), $\text{NiSO}_4 \cdot 6\text{H}_2\text{O}$ (0.20 mmol, 0.052 g), NaOH (0.20 mmol, 0.008 g), and 15 mL H_2O was sealed in a Teflon-lined stainless steel vessel, heated to 170 $^\circ\text{C}$ for 3 days, and followed by slow cooling (a descent rate of 10 $^\circ\text{C/h}$) to room temperature. The green block crystals of **1** were obtained. Yield of 71% (based on Ni). Anal. (%) calcd. for $\text{C}_{25}\text{H}_{21}\text{N}_4\text{NiO}_5$ (516.15): C, 58.17; H, 4.10; N, 10.85. Found: C, 57.97; H, 4.32; N, 10.56. IR (KBr pellet, cm^{-1}): 3445 (vs), 3070 (vs), 1702 (vs), 1579 (vs), 1421 (vs), 1389 (vs), 1229 (s), 1145 (s), 853 (s), 726 (s), 652 (w).

Synthesis of $[\text{Mn}(\text{tptc})_{0.5}(\text{1,3-bimb})(\text{H}_2\text{O})_n]_n$ (2**).** A mixture of H_4tptc (0.10 mmol, 0.033 g), 1,3-bimb (0.30 mmol, 0.071 g), $\text{MnSO}_4 \cdot \text{H}_2\text{O}$ (0.30 mmol, 0.051 g), NaOH (0.30 mmol, 0.012 g), and 14 mL H_2O was sealed in a Teflon-lined stainless steel vessel, heated to 170 $^\circ\text{C}$ for 3 days, and followed by slow cooling (a descent rate of 10 $^\circ\text{C/h}$) to room temperature. The colorless block crystals of **2** were obtained. Yield of 63% (based on Mn). Anal. (%) calcd. for $\text{C}_{25}\text{H}_{21}\text{MnN}_4\text{O}_5$ (512.40): C, 58.60; H, 4.13; N, 10.93. Found: C, 58.26; H, 4.34; N, 10.77. IR (KBr pellet, cm^{-1}): 3421 (s), 3058 (s), 1699 (s), 1608 (s), 1517 (s), 1578 (vs), 1542 (vs), 1358 (vs), 1257 (m), 1160 (m), 827 (w), 723 (m), 638 (w).

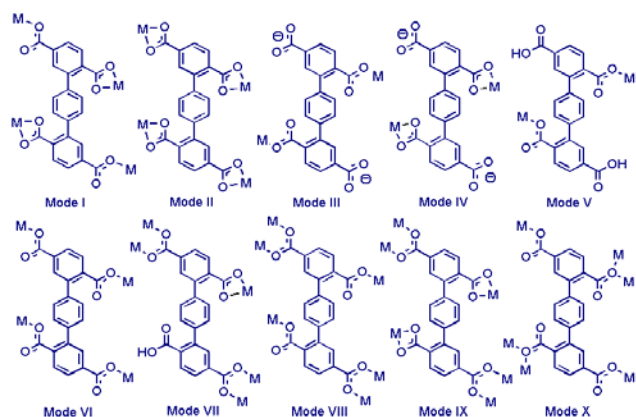
Synthesis of $\{[\text{Ni}(\text{tptc})_{0.5}(\text{1,4-bmib})] \cdot 0.25\text{H}_2\text{O}\}_n$ (3**).** A mixture of H_4tptc (0.15 mmol, 0.050 g), 1,4-bmib (0.40 mmol, 0.106 g), $\text{NiSO}_4 \cdot 6\text{H}_2\text{O}$ (0.10 mmol, 0.026 g), NaOH (0.40 mmol, 0.016 g), and 15 mL H_2O was sealed in a Teflon-lined stainless steel vessel, heated to 170 $^\circ\text{C}$ for 3 days, followed by slow cooling (a descent rate of 10 $^\circ\text{C/h}$) to room temperature. The green block crystals of **3** were obtained. Yield of 54% (based on

Ni). Anal. (%) calcd. for $\text{C}_{27}\text{H}_{23.5}\text{N}_4\text{NiO}_{4.25}$ (530.69): C, 61.11; H, 4.46; N, 10.56. Found: C, 60.78; H, 4.71; N, 10.63. IR (KBr pellet, cm^{-1}): 3423 (s), 3018 (vs), 1698 (m), 1585 (m), 1422 (vs), 1371 (vs), 1286 (s), 1141 (s), 862 (vs), 744 (m), 667 (w).

Synthesis of $\{[\text{Ni}(\text{tptc})_{0.5}(\text{4,4'-bibp})_2(\text{H}_2\text{O})] \cdot 2\text{H}_2\text{O}\}_n$ (4**).** A mixture of H_4tptc (0.15 mmol, 0.050 g), 4,4'-bibp (0.30 mmol, 0.086 g), $\text{NiCl}_4 \cdot 6\text{H}_2\text{O}$ (0.30 mmol, 0.060 g), and 15 mL H_2O was adjust to the pH ≈ 7 with 1M NaOH, sealed in a Teflon-lined stainless steel vessel, heated to 170 $^\circ\text{C}$ for 3 days, and followed by slow cooling (a descent rate of 10 $^\circ\text{C/h}$) to room temperature. Green block crystals of **4** were obtained. Yield of 51% (based on Ni). Anal. (%) calcd. for $\text{C}_{47}\text{H}_{37}\text{N}_8\text{NiO}_6$ (886.57): C, 65.00; H, 4.29; N, 12.90. Found: C, 64.63; H, 4.51; N, 12.69. IR (KBr pellet, cm^{-1}): 3467 (m), 3139 (vs), 1574 (vs), 1405 (s), 1352 (vs), 1310 (s), 1123 (s), 849 (m), 721 (m), 658 (w).

Synthesis of $\{[\text{Ni}(\text{tptc})_{0.5}(\text{4,4'-bimbp})_{1.5}(\text{H}_2\text{O})] \cdot \text{H}_2\text{O}\}_n$ (5**).** The synthetic method is similar to that of compound **4** except that 4,4'-bimbp replaced 4,4'-bibp. Green block were obtained after cooling to room temperature with the yield of 67% (based on Ni). Anal. (%) calcd. for $\text{C}_{41}\text{H}_{36}\text{N}_6\text{NiO}_6$ (767.47): C, 64.17; H, 4.73; N, 10.95. Found: C, 63.92; H, 4.91; N, 10.77. IR (KBr pellet, cm^{-1}): 3369 (s), 3139 (m), 1676 (m), 1592 (vs), 1514 (s), 1361 (vs), 1231 (m), 1109 (m), 823 (s), 750 (m), 661 (m).

X-ray Crystallography. Intensity data collection was carried out on a Siemens SMART diffractometer equipped with a CCD detector using Mo-K α monochromatized radiation ($\lambda=0.71073\text{\AA}$) at 293(2) or 296(2) K. The absorption correction was based on multiple and symmetry-equivalent reflections in the data set using the SADABS program based on the method of Blessing. The structures were solved by direct methods and refined by full-matrix least-squares using the SHELXTL package.¹¹ All non-hydrogen atoms were refined anisotropically. Hydrogen atoms except those for water molecules were generated geometrically with fixed isotropic thermal parameters, and included in the structure factor calculations. The approximate positions of the water H atoms, obtained from a difference Fourier map, were restrained to ideal configuration of the water molecule and fixed in the final stages of refinement. Four carbon atoms in one phenyl ring of 4,4'-bibp in compound **4** and 4,4'-bimbp in compound **5** are disordered and were refined with split positions and an occupancy ratio of 45:55 for **4**, 49.1:50.9 for **5**, respectively. Crystallographic data for compounds **1–5** are given in Table 1. Selected bond lengths and angles are listed in Table 2. For complexes of **1–5**, further details on the crystal structure investigations can be obtained from the Cambridge Crystallographic Data Centre, CCDC, 12 Union Road, CAMBRIDGE CB2 1EZ, UK, [Telephone: +44-(0)1223-762-910, Fax: +44-(0)1223-336-033; Email: deposit@ccdc.cam.ac.uk, <http://www.ccdc.cam.ac.uk/deposit/>], on quoting the depository number CCDC-973827 for **1**, 973828 for **2**, 973829 for **3**, 973830 for **4**, and 973831 for **5**.



Scheme 1. The coordination modes of H_4tptc in complexes **1-5** and references.

Result and Discussion

Synthesis and Characterization. Compounds **1-5** were obtained by the solvothermal reactions of H_4tptc , transition metal cations (Ni^{II} , Mn^{II}) and related bis(imidazole) bridging ligands at 170 °C. All complexes are insoluble in water and common organic solvents including methanol, ethanol, chloroform, toluene, and acetonitrile.

The IR spectra of **1-5** are similar. The absorption bands in the range of 3400-3500 cm^{-1} for **1-5** can be attributed to the characteristic peaks of water O-H vibrations. The vibrations at ca. 1530 and 1565 cm^{-1} correspond to the asymmetric and symmetric stretching vibrations of the carboxylate groups, respectively (Fig. S1). The absence of strong absorption bands from 1300 to 1600 cm^{-1} proves that H_4tptc ligands are completely deprotonated.¹²

Structure descriptions of $[M(tptc)_{0.5}(1,3-bimb)(H_2O)]_n$ ($M = Ni$ for **1, Mn for **2**).** The single-crystal X-ray diffraction analyses reveal that complexes **1** and **2** are isomorphous and crystallize in the monoclinic system, $C2/c$ space group, herein only the structure of **1** will be discussed as a representation. The asymmetric unit of **1** contains one crystallographically independent Ni^{II} ion, a half of $tptc^{4-}$ ligand, one 1,3-bimb ligand, and one associated water molecule, shown in Fig 1a. In compound **1**, the carboxylate groups of $tptc^{4-}$ are completely deprotonated and show the $(\kappa^1-\kappa^0)-(\kappa^1-\kappa^1)-(\kappa^1-\kappa^0)-(\kappa^1-\kappa^1)-\mu_4$ coordination mode (Mode I, Scheme 1). Each Ni^{II} ion is hexacoordinated by four oxygen atoms from two $tptc^{4-}$ ligands, one coordinated water molecule, and two nitrogen atoms from two 1,3-bimb ligands. The bond lengths of Ni–O are in the range of 2.055(4)–2.142(3) Å, and the Ni–N bond distances are 2.035(4) and 2.097(4) Å, respectively. The dihedral angles between central phenyl ring and the two outer ones are equal (41.31°), and the dihedral angle between two terminal benzene rings is 82.63°, which indicates that the $tptc^{4-}$ was seriously distorted and extremely unsymmetrical.

The μ_4-tptc^{4-} ligand connected four Ni^{II} ions forming one $[Ni_2(tptc)]_n$ sheet, in which left-handed helical chains occupied (Fig. 1b). The $[Ni_2(tptc)_2]_n$ layers were further linked by the $[Ni(1,3-bimb)]_2$ loops (Fig. S2) forming one 3D framework (Fig. 1c). With guest water molecules being omitted, calculation PLATON shows that the void volume of **1** is 4.3 % of the crystal volume (205.5 out of the 4739.0 Å³ unit cell volumes).¹³

The topological analysis method was accessed to simplify the structure.¹⁴ The overall framework can be defined as a binodal (3,4)-connected $t\bar{f}i$ nets with the point Schläfli symbol of $(4\cdot6^2)(4\cdot6^6\cdot8^3)$ (Fig. 1d) by denoting the Ni^{II} and $tptc^{4-}$ as 4-connected and 3-connected nodes, respectively (Fig. 1d).

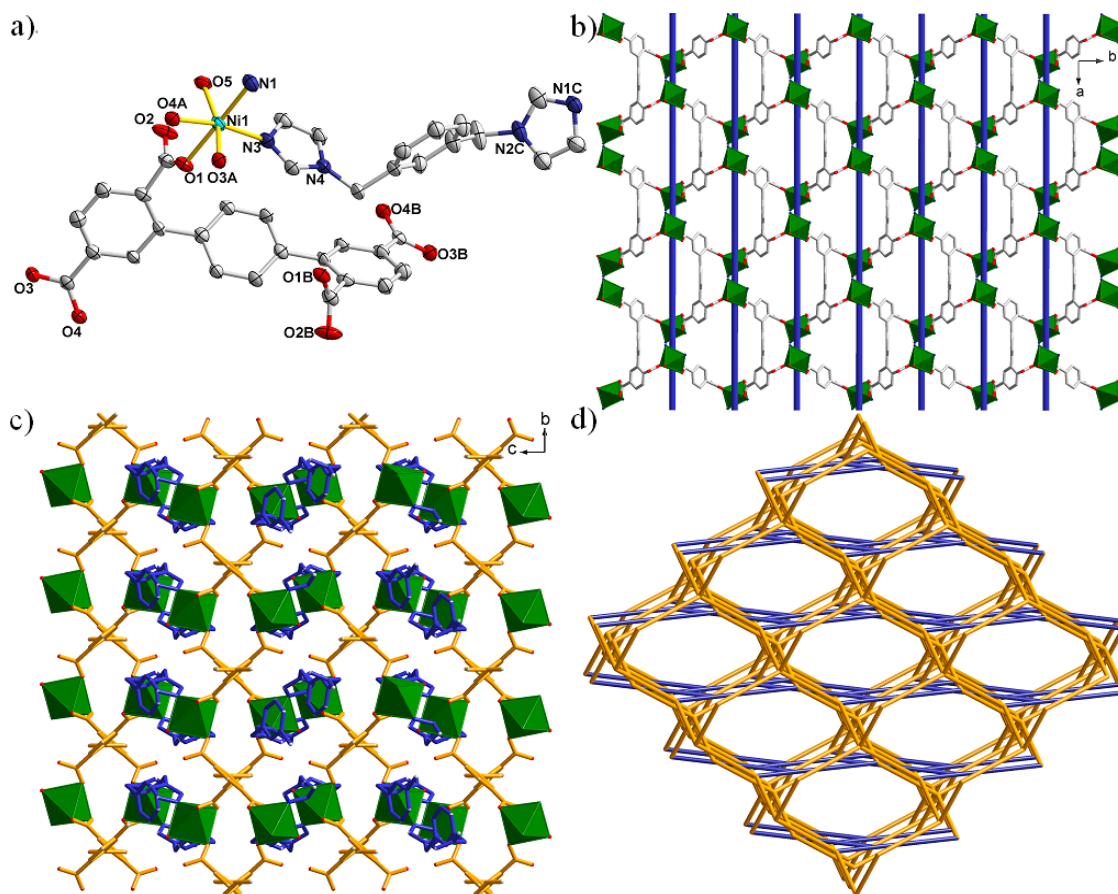


Fig. 1 (a) Coordination environment of Ni^{II} atom in **1** with thermal ellipsoids at 50% probability level (Symmetry codes: A 1.5-x, 0.5+y, 0.5-z; B 1-x, y, 0.5-z; C 0.5-x, 0.5-y, 1-z). (b) View of the 2D [Ni₂(tpc)]_n sheet with right- and left-handed helices. (c) View of the 3D frameworks of compound **1**. (d) Schematic view of the 3D architecture exhibits a binodal (3,4)-connected **tff** nets with the point Schläfli symbol of (4·6²)(4·6⁶·8³) (Gold bonds: tpc⁴⁻ ligands; Dark blue bonds: 1,3-bimb ligands).

Table 1 Crystal data for **1** – **5**.

Compound	1	2	3	4	5
Empirical formula	C ₂₅ H ₂₁ N ₄ NiO ₅	C ₂₅ H ₂₁ MnN ₄ O ₅	C ₂₇ H _{23.5} N ₄ NiO _{4.25}	C ₄₇ H ₃₇ N ₈ NiO ₆	C ₄₁ H ₃₆ N ₆ NiO ₆
Formula weight	516.17	512.40	530.69	868.56	767.47
Crystal system	Monoclinic	Monoclinic	Monoclinic	Triclinic	Triclinic
Space group	C2/c	C2/c	C2/c	P-1	P-1
<i>a</i> (Å)	17.073(11)	16.3353(12)	16.388(7)	11.9535(5)	12.785(3)
<i>b</i> (Å)	15.507(11)	16.0464(12)	16.225(7)	12.9115(6)	13.443(4)
<i>c</i> (Å)	18.110(12)	18.4433(15)	19.438(8)	13.8933(6)	14.029(4)
<i>α</i> (°)	90	90	90	83.9270(10)	96.636(4)
<i>β</i> (°)	98.765(13)	101.6790(10)	95.373(7)	80.9780(10)	114.001(4)
<i>γ</i> (°)	90	90	90	86.0030(10)	115.893(4)
<i>V</i> (Å ³)	4739(5)	4734.3(6)	5146(4)	2102.76(16)	1851.2(8)
<i>Z</i>	8	8	8	2	2
<i>D</i> _{calc} (g/cm ³)	1.447	1.438	1.370	1.372	1.377
<i>μ</i> (mm ⁻¹)	0.863	0.602	0.795	0.522	0.581
<i>T</i> (K)	296(2)	296(2)	296(2)	293(2)	296(2)
<i>θ</i> range (°)	2.01–25.00	1.80–25.00	1.77–25.05	2.28–25.25	1.70–25.25
Data/Parameters	4129/322	4167/322	4554/329	7575/584	6660/512
<i>F</i> (000)	2136	2112	2204	902	800
<i>R</i> _{int}	0.0740	0.0239	0.0273	0.0184	0.0227
Final <i>R</i> indices [<i>I</i> > 2σ(<i>I</i>)]	<i>R</i> ₁ = 0.0623 <i>wR</i> ₂ = 0.1509	<i>R</i> ₁ = 0.0328 <i>wR</i> ₂ = 0.0857	<i>R</i> ₁ = 0.0385 <i>wR</i> ₂ = 0.1164	<i>R</i> ₁ = 0.0639 <i>wR</i> ₂ = 0.1673	<i>R</i> ₁ = 0.0529 <i>wR</i> ₂ = 0.1317
<i>R</i> indices (all data)	<i>R</i> ₁ = 0.1002 <i>wR</i> ₂ = 0.1740	<i>R</i> ₁ = 0.0427 <i>wR</i> ₂ = 0.0928	<i>R</i> ₁ = 0.0483 <i>wR</i> ₂ = 0.1248	<i>R</i> ₁ = 0.0775 <i>wR</i> ₂ = 0.1801	<i>R</i> ₁ = 0.0793 <i>wR</i> ₂ = 0.1490
Gof	1.001	0.999	1.001	1.002	1.001
$R_1 = \sum F_o - F_c / \sum F_o $, $wR_2 = [\sum w(F_o^2 - F_c^2)^2] / \sum w(F_o^2)^{1/2}$					

Table 2 Selected bond lengths (Å) and angles (°) for **1 – 5**.

Complex 1							
N(1)-Ni(1)	2.035(4)	N(3)-Ni(1)	2.097(4)	Ni(1)-O(5)	2.055(4)	Ni(1)-O(1)	2.092(3)
Ni(1)-O(4) ^{#1}	2.117(4)	Ni(1)-O(3) ^{#1}	2.142(3)	N(1)-Ni(1)-O(5)	94.60(15)	N(1)-Ni(1)-O(1)	91.85(16)
O(5)-Ni(1)-O(1)	90.80(14)	N(1)-Ni(1)-N(3)	89.39(17)	O(5)-Ni(1)-N(3)	89.46(17)	O(1)-Ni(1)-N(3)	178.71(15)
N(1)-Ni(1)-O(4) ^{#1}	100.88(15)	O(5)-Ni(1)-O(4) ^{#1}	164.52(13)	O(1)-Ni(1)-O(4) ^{#1}	88.62(14)	N(3)-Ni(1)-O(4) ^{#1}	90.80(17)
N(1)-Ni(1)-O(3) ^{#1}	162.90(15)	O(5)-Ni(1)-O(3) ^{#1}	102.51(13)	O(1)-Ni(1)-O(3) ^{#1}	87.75(14)	O(4) ^{#1} -Ni(1)-O(3) ^{#1}	62.01(13)
N(3)-Ni(1)-O(3) ^{#1}	90.96(15)	Symmetry codes: #1 -x+3/2, y+1/2, -z+1/2.					
Complex 2							
Mn(1)-O(1) ^{#1}	2.1503(14)	Mn(1)-O(1W)	2.1655(15)	Mn(1)-N(1)	2.1808(17)	Mn(1)-O(3)	2.2508(13)
Mn(1)-N(4)	2.2765(19)	Mn(1)-O(4)	2.3056(15)	O(1) ^{#1} -Mn(1)-N(1)	95.58(6)	O(1W)-Mn(1)-N(1)	95.67(6)
O(1) ^{#1} -Mn(1)-O(3)	87.35(5)	O(1W)-Mn(1)-O(3)	111.34(5)	N(1)-Mn(1)-O(3)	152.93(6)	O(1) ^{#1} -Mn(1)-N(4)	174.27(6)
O(1W)-Mn(1)-N(4)	88.15(6)	N(1)-Mn(1)-N(4)	89.10(7)	O(3)-Mn(1)-N(4)	89.98(6)	O(1) ^{#1} -Mn(1)-O(4)	93.81(6)
O(1W)-Mn(1)-O(4)	168.65(5)	N(1)-Mn(1)-O(4)	95.28(6)	O(3)-Mn(1)-O(4)	57.65(5)	O(1) ^{#1} -Mn(1)-O(1W)	88.10(5)
N(4)-Mn(1)-O(4)	89.04(6)	Symmetry codes: #1 -x+1/2, y-1/2, -z+1/2.					
Complex 3							
N(1)-Ni(1)	2.024(2)	N(3)-Ni(1)	2.039(2)	Ni(1)-O(4) ^{#1}	2.067(2)	Ni(1)-O(2)	2.104(2)
Ni(1)-O(1)	2.130(2)	Ni(1)-O(3) ^{#1}	2.216(2)	N(1)-Ni(1)-N(3)	95.59(10)	N(1)-Ni(1)-O(4) ^{#1}	95.55(9)
N(3)-Ni(1)-O(4) ^{#1}	95.69(9)	N(1)-Ni(1)-O(2)	103.03(9)	N(3)-Ni(1)-O(2)	95.73(9)	O(4) ^{#1} -Ni(1)-O(2)	157.08(8)
N(1)-Ni(1)-O(1)	164.88(9)	N(3)-Ni(1)-O(1)	89.09(9)	O(4) ^{#1} -Ni(1)-O(1)	98.29(8)	O(2)-Ni(1)-O(1)	62.12(7)
N(1)-Ni(1)-O(3) ^{#1}	89.07(9)	N(3)-Ni(1)-O(3) ^{#1}	156.76(8)	O(4) ^{#1} -Ni(1)-O(3) ^{#1}	61.15(8)	O(1)-Ni(1)-O(3) ^{#1}	92.27(8)
O(2)-Ni(1)-O(3) ^{#1}	105.39(8)	Symmetry codes: #1 x, -y+1, z-1/2.					
Complex 4							
Ni(1)-O(1)	2.070(10)	Ni(1)-N(5)	2.078(13)	Ni(1)-N(3)	2.081(13)	Ni(1)-N(1)	2.121(13)
Ni(1)-N(8) ^{#1}	2.128(14)	Ni(1)-O(1W)	2.141(11)	O(1)-Ni(1)-N(5)	176.0(5)	O(1)-Ni(1)-N(3)	87.5(5)
N(5)-Ni(1)-N(3)	91.6(5)	O(1)-Ni(1)-N(1)	86.0(5)	N(5)-Ni(1)-N(1)	98.0(5)	N(3)-Ni(1)-N(1)	90.2(5)
O(1)-Ni(1)-N(8) ^{#1}	86.2(5)	N(5)-Ni(1)-N(8) ^{#1}	95.0(5)	N(3)-Ni(1)-N(8) ^{#1}	171.9(5)	N(1)-Ni(1)-N(8) ^{#1}	84.3(5)
O(1)-Ni(1)-O(1W)	87.7(4)	N(5)-Ni(1)-O(1W)	88.4(5)	N(3)-Ni(1)-O(1W)	88.0(5)	N(8) ^{#1} -Ni(1)-O(1W)	96.9(5)
N(1)-Ni(1)-O(1W)	173.4(5)	Symmetry codes: #1 x-1, y, z+1.					
Complex 5							
N(1)-Ni(1)	2.091(3)	N(5)-Ni(1)	2.037(3)	Ni(1)-N(4) ^{#1}	2.079(4)	Ni(1)-O(1W)	2.091(3)
Ni(1)-O(2)	2.113(3)	Ni(1)-O(1)	2.172(3)	N(5)-Ni(1)-N(4) ^{#1}	89.14(14)	N(5)-Ni(1)-O(1W)	99.72(13)
O(1W)-Ni(1)-O(1)	100.49(11)	N(1)-Ni(1)-O(1)	89.66(12)	N(4) ^{#1} -Ni(1)-O(1W)	89.19(13)	N(5)-Ni(1)-N(1)	90.61(14)
N(4) ^{#1} -Ni(1)-N(1)	176.24(14)	O(1W)-Ni(1)-N(1)	87.15(13)	N(5)-Ni(1)-O(2)	98.06(12)	N(4) ^{#3} -Ni(1)-O(2)	91.45(13)
O(1W)-Ni(1)-O(2)	162.22(12)	N(1)-Ni(1)-O(2)	92.30(13)	N(5)-Ni(1)-O(1)	159.77(12)	N(4) ^{#3} -Ni(1)-O(1)	91.87(13)
O(2)-Ni(1)-O(1)	61.72(11)	Symmetry codes: #1 -x+1, -y+2, -z+2.					

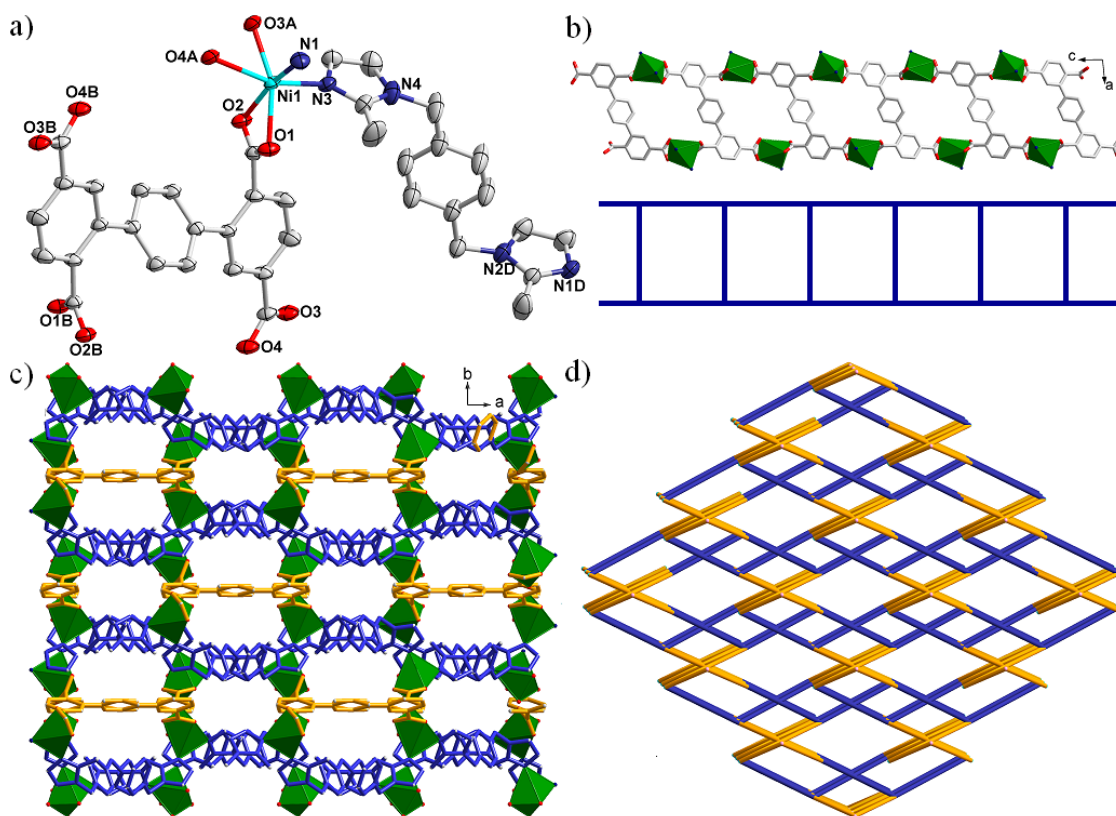


Fig. 2 (a) Coordination environment of Ni^{II} atom in **3** with thermal ellipsoids at 50% probability level (Symmetry codes: A $x, 1-y, -0.5+z$; B $1-x, 1-y, 1-z$; D $-0.5+x, 0.5-y, 0.5+z$). (b) View of the 1D $[\text{Ni}_2(\text{tpc})]_n$ chains along b axis. (c) View of the 3D frameworks of compound **3**. (d) Schematic view of the novel (4,4)-connected frameworks with the Point Schläfli symbol of $(4^6 \cdot 6^2)_2(4^2 \cdot 8^4)$ (Gold bonds: tpc^{4-} ligands; Dark blue bonds: 1,4-bnmb ligands).

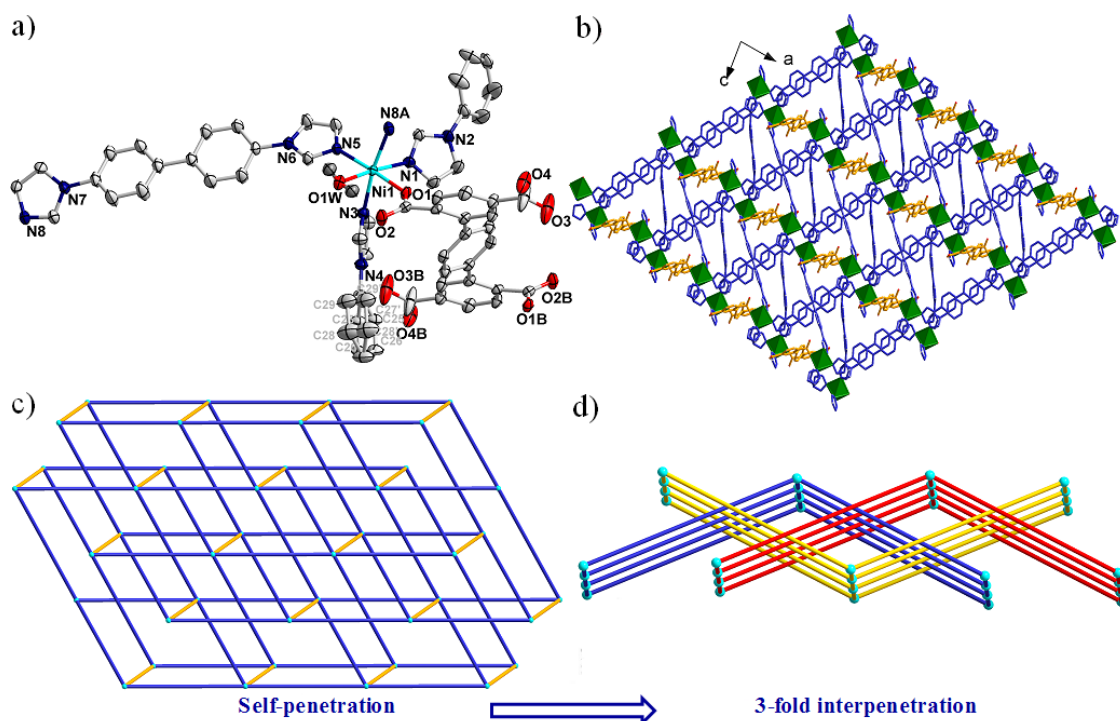


Fig. 3 (a) Coordination environment of Ni^{II} atom in **4** with thermal ellipsoids at 50% probability level (Symmetry codes: A $-1+x, y, 1+z$; B $-x, -y, 1-z$). (b) View of the 2D networks of compound **4**. (c) Schematic view of the novel 5-connected networks with the Point Schläfli symbol of $(4^6 \cdot 6^4)$ (Gold bonds: tpc^{4-} ligands; Dark blue bonds: 4,4'-bibp ligands). (d) Simplified 3-fold $(4^4 \cdot 6^2)$ -**sql** interpenetrating networks after breaking the Ni-O bonds.

Structure descriptions of $\{[\text{Ni}(\text{tptc})_{0.5}(1,4\text{-bmib})]\cdot 0.25\text{H}_2\text{O}\}_n$ (3**).** The single-crystal X-ray diffraction analysis reveals that complex **3** crystallizes in the monoclinic system, $C2/c$ space group. As shown in Fig. 2a, there are one Ni^{II} ion, a half of tptc^{4-} ligand, one 1,4-bmib ligand, and a quarter of a coordinated water molecules in the asymmetric unit. The Ni^{II} cation is coordinated by four oxygen atoms from two tptc^{4-} ligands and two nitrogen atoms from two individual 1,4-bmib ligands, leaving a distorted octahedral geometry. The bond lengths of Ni–O are in the range of 2.067(2)–2.216(2) Å, and the Ni–N bond distances are 2.024(2) and 2.039(2) Å, respectively. The dihedral angles between the central phenyl ring and two neighbouring phenyl rings are equal (34.91°). The one between two terminal phenyl rings is 0.00°, which indicated the two terminal phenyl rings are paralleled to each other.

Different from the one in **1** and **2**, tptc^{4-} exhibits $(\kappa^1-\kappa^1)-(\kappa^1-\kappa^1)-(\kappa^1-\kappa^1)-\mu_4$ coordination mode in complex **3** (Mode II). Four Ni^{II} ions are connected by $\mu_4\text{-tptc}^{4-}$ to form one ladder $[\text{Ni}_2(\text{tptc})]_n$ structure along c axis (Fig. 2b), which are linked by 1,4-bmib ligands along two different directions to exhibit a 3D framework (Fig. 2c). The effective free volume of **3** was 7.8% of the crystal volume (400.1 out of the 5146.0 Å³ unit cell volumes), calculated by PLATON analysis.

From a topology view, the overall framework can be defined as a novel (4,4)-connected framework with the Schläfli symbol $(4.6^4.8)_2(4^2.8^4)$ by denoting Ni^{II} ions and tptc^{4-} as 4-connected nodes and 1,4-bmib as 2-connected nodes, respectively (Fig. 2d).

Structure descriptions of $\{[\text{Ni}(\text{tptc})_{0.5}(4,4'\text{-bibp})_2(\text{H}_2\text{O})]\cdot 2\text{H}_2\text{O}\}_n$ (4**).** X-ray crystallographic analysis shows that complex **4** is a novel 5-connected 2D network with the Schläfli symbol of $(4^6.6^4)$. Complex **4** crystallizes in the triclinic system, $P-1$ space group. The asymmetric unit contains one Ni^{II} ion, a half of tptc^{4-} ligand, two 4,4'-bibp ligands, and one coordinated and two lattice water molecules. As shown in Fig. 3a, each Ni^{II} ion is located in a distorted octahedral coordination environment, completed by two oxygen atoms from one tptc^{4-} ligand, one coordinated water molecule, and four nitrogen atoms from four individual 4,4'-bibp ligands. The Ni–N bond distances are in the range of 2.078(13)–2.128(14) Å and the Ni–O bond distances are 2.070(10) and 2.141(11) Å, respectively.

Although tptc^{4-} ligands in complex **4** are completely deprotonated, only two carboxylate groups took part in coordination with Ni^{II} ions by adopting $(\kappa^1-\kappa^0)-\mu_1$ coordination mode (Mode III). Ni^{II} ions are connected by 4,4'-bibp ligands forming 2D $[\text{Ni}(4,4'\text{-bibp})]_n$ polymeric layer (Fig. S4), which contains big square circles built from four Ni^{II} ions and four 4,4'-bibp ligands. More interestingly, three 2D $[\text{Ni}(4,4'\text{-bibp})]_n$ polymeric layers are self-penetrated with each other. And the tptc^{4-} ligands only act as the role of solidification to the self-penetration by coordination to nickel ions from two 2D $[\text{Ni}(4,4'\text{-bibp})]_n$ polymeric layers (Fig. 3b). Furthermore, neighboring layers stack in a parallel fashion along the crystal [010] direction giving rise to a 3D supramolecular framework *via* inter-layer O–H...O hydrogen bonds [O5–H2...O4ⁱ, O5–H2...O2, and O5–H1...O1]. Symmetry codes: (i) $-x, -y+1, -z+1$ between coordinated water molecules and the deprotonated carboxylate groups of tptc^{4-} ligands.

At the sight of topology, the final framework can be defined as a novel 5-connected net with the Schläfli symbol of $(4^6.6^4)$ (Fig. 3c). It is worth noting that the 2D $[\text{Ni}(4,4'\text{-bibp})]_n$ polymeric layer can be easily decomposed to three interpenetrating 2D $(4^4.6^2)\text{-sql}$ nets by breaking the Ni–O bonds (Fig. 3d).

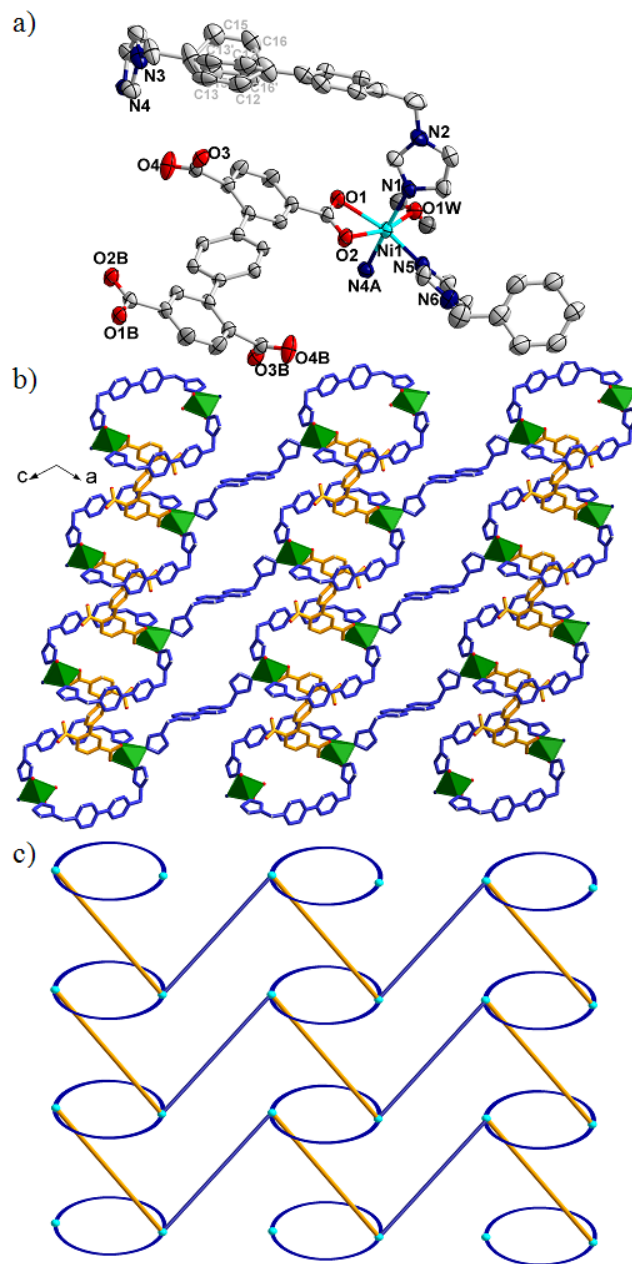


Fig. 4 (a) Coordination environment of Ni^{II} atom in **5** with thermal ellipsoids at 50% probability level (Symmetry codes: A $1-x, 2-y, 2-z$; B $-x, 2-y, 1-z$). (b) View of the 2D polymeric layer of compound **5**. (c) Schematic view of the 6^3-hcb network (Gold bonds: tptc^{4-} ligands; Dark blue bonds: 4,4'-bibp ligands).

Structure descriptions of $\{[\text{Ni}(\text{tptc})_{0.5}(4,4'\text{-bibp})_{1.5}(\text{H}_2\text{O})]\cdot \text{H}_2\text{O}\}_n$ (5**).** Structural analysis indicates that complex **5** crystallizes in the triclinic system, $P-1$ space group. The asymmetric unit of **5** is composed of one Ni^{II} ion, a half of tptc^{4-} ligand, one and a half of 4,4'-bibp ligands, one coordinated and one lattice water molecules. The Ni^{II} ion is

located in a slightly distorted NiO_3N_3 octahedral coordination geometry completed by three N atoms belonging to three 4,4'-bimbp ligands, three O atoms from two tptc^{4-} ligands, and one coordinated water molecule, shown in Fig. 4a. The Ni–O bond distances are in the range of 2.091(3)–2.172(3) Å and the Ni–N bond distances are vary from 2.037(3) to 2.091(3) Å, respectively.

Similar to complex **4**, the tptc^{4-} in complex **5** also coordinated with two Ni^{II} ions with $(\kappa^1-\kappa^1)-\mu_1$ cheating carboxylate groups (Mode IV). Each two Ni^{II} ions are coordinated by two 4,4'-bimbp

ligands forming one approximately circularity $[\text{Ni}_2(4,4'\text{-bimbp})_2]$ metallamacrocyclic, which are further linked by another 4,4'-bimbp, exhibiting the interesting 1D $[\text{Ni}_2(4,4'\text{-bimbp})_3]_n$ chain with loops. Based on which, a 2D polymeric layer was constructed with the help of tptc^{4-} (Fig. 4b). The neighboring layers are all held together by classical O–H...O hydrogen bonds to form a 3D supramolecular framework. The whole structure can be view as a 6^3-hcb net by donating the Ni^{II} ions to a 3-connected nodes, and all the organic ligands as linkers (Fig. 4c).

Table 3 The coordination modes of H_4tptc ligand, ancillary ligands, dihedral angles, topology, and structure in complexes **1–5** and references.

Compound	CoordinationMode	Ancillary ligands	Dihedral Angles (°)	Topology	Structure
Compound 1	Mode I	1,3-bimb/bridging	41.3(1),82.6(3),41.3(1)	$(4\cdot6^2)(4\cdot6\cdot8^3)$	3D (3,4)-connected nets
Compound 2	Mode I	1,3-bimb/bridging	39.5(3),79.0(6),39.5(3)	$(4\cdot6^2)(4\cdot6\cdot8^3)$	3D (3,4)-connected nets
Compound 3	Mode II	1,4-bimb/bridging	34.9(1),0.0(0),34.9(1)	$(4\cdot6^4\cdot8^2)(4^2\cdot8^4)$	3D (4,4)-connected nets
Compound 4	Mode III	4,4'-bimb/bridging	40.7(4),0.0(0),40.7(4)	$(4^6\cdot6^4)$	2D 5-connected nets
Compound 5	Mode IV	4,4'-bimb/bridging	36.0(7),0.0(0),36.0(7)	(6^3)	2D 3-connected nets
$\text{Co}(\text{H}_2\text{qptc})(\text{phen})^{15a}$	Mode V	phen/chelating	39.7(7),0.0(0),39.7(7)	N/A	1D zigzag chain
$\text{Ni}(\text{H}_2\text{qptc})(\text{phen})^{15a}$	Mode V	phen/chelating	40.0(4),0.0(0),40.0(4)	N/A	1D zigzag chain
$\text{Mn}(\text{qptc})_{0.5}(\text{phen})^{15a}$	Mode X	phen/chelating	42.2(4),0.0(0),42.2(4)	$(4^3)_2(4^6\cdot6\cdot8^3)$	2D (3,6)-connected nets
$\text{Cu}(\text{qptc})_{0.5}(\text{phen})^{15a}$	Mode IX	phen/chelating	46.6(7),87.6(7),46.6(7)	$(4^2\cdot6)_2(4^4\cdot6^2\cdot8^8\cdot10)$	3D (3,6)-connected nets
$\text{Zn}_3(\text{Hqptc})_2(\text{phen})_2^{15a}$	Mode VII	phen/chelating	38.7(2),85.7(0),55.9(3)	$(4^2\cdot6)_2(4^3\cdot6^2\cdot8)(4^5\cdot6^4\cdot8)_2$	3D (3,4,5)-connected nets
$\text{Co}(\text{qptc})_{0.5}(2,2'\text{-bpy})^{15b}$	Mode VIII	2,2-bpy/chelating	45.3(1),0.0(0),45.3(1)	$(4^3)_2(4^6\cdot6\cdot8^3)$	2D (3,6)-connected nets
$\text{Ni}(\text{qptc})_{0.5}(2,2'\text{-bpy})^{15b}$	Mode VIII	2,2-bpy/chelating	46.8(6),0.0(0),46.8(6)	$(4^3)_2(4^6\cdot6\cdot8^3)$	2D (3,6)-connected nets
$\text{Cu}(\text{H}_2\text{qptc})(2,2'\text{-bpy})^{15b}$	Mode V	2,2-bpy/chelating	44.8(8),0.0(0),44.8(8)	N/A	1D zigzag chain
$\text{Mn}(\text{qptc})_{0.5}(2\text{-bpz})^{15c}$	Mode VI	2-bpz/chelating	38.7(0),0.0(0),38.7(0)	$(4^4\cdot6^2)$	2D 4-connected nets
$\text{Ni}(\text{H}_2\text{qptc})(4,4'\text{-bpy})^{15d}$	Mode V	4,4-bpy/bridging	41.1(5),0.0(0),41.1(5)	N/A	1D zigzag chain
$\text{Zn}_2(\text{qptc})(4,4'\text{-bpy})^{15d}$	Mode VI	4,4-bpy/bridging	51.8(6),0.0(0),51.8(6)	$(4^2\cdot6)_2(4^3\cdot6^2\cdot8)(4^5\cdot6^4\cdot8)_2$	3D (3,4)-connected nets
$\text{Ni}(\text{qptc})_{0.5}(4,4'\text{-bpe})^{15f}$	Mode VI	4,4-bpe/bridging	51.1(6),0.0(0),51.1(6)	$(6^2\cdot8^4)(6^2\cdot8)_2$	3D (3,4)-connected nets
$\text{Mn}(\text{qptc})(\text{dppf-O})^{15c}$	Mode VI	dppf-O/bridging	43.0(2),0.0(0),43.0(2)	$(5^4\cdot6^2)(5^{10}\cdot6^3\cdot7\cdot8)$	3D (4,6)-connected nets
$\text{Fe}(\text{qptc})(\text{dppf-O})^{15c}$	Mode VI	dppf-O/bridging	45.0(5),0.0(0),45.0(5)	$(5^4\cdot6^2)(5^{10}\cdot6^3\cdot7\cdot8)$	3D (4,6)-connected nets

Note: all the solvent molecules were omitted from the formulas. Abbreviation: phen=phenanthroline; 2,2'-bpy=2,2'-bipyridine; 2-bpz=3-(2-pyridyl)pyrazole; 4,4'-bpy=4,4'-bipyridine; 4,4'-bpe=1, 3-bis(4-pyridyl)propane; dppf=1,2-bis(diphenylphosphino)ethane.

Structural Discussion. As shown in Scheme 1 and Table 3, H_4tptc exhibits versatile coordination modes including $(\kappa^1-\kappa^1)-(\kappa^1-\kappa^0)-(\kappa^1-\kappa^1)-(\kappa^1-\kappa^0)-\mu_4$ (Mode I, in **1** and **2**), $(\kappa^1-\kappa^1)-(\kappa^1-\kappa^1)-\mu_4$ (Mode II, in **3**), $(\kappa^1-\kappa^0)-\mu_1$ (Mode III, in **4**), $(\kappa^1-\kappa^1)-\mu_1$ (Mode IV, in **5**), $(\kappa^1-\kappa^0)-\mu_1$ (Mode V), $^{15a, b, d}$ $(\kappa^1-\kappa^0)-(\kappa^1-\kappa^0)-(\kappa^1-\kappa^0)-(\kappa^1-\kappa^0)-\mu_4$ (Mode VI), $^{15c-e}$ $(\kappa^1-\kappa^1)-(\kappa^1-\kappa^1)-(\kappa^1-\kappa^1)-\mu_5$ (Mode VII), 15a $(\kappa^1-\kappa^1)-(\kappa^1-\kappa^0)-(\kappa^1-\kappa^1)-(\kappa^1-\kappa^0)-\mu_6$ (Mode VIII), 15b $(\kappa^1-\kappa^1)-(\kappa^1-\kappa^1)-(\kappa^1-\kappa^1)-(\kappa^1-\kappa^1)-\mu_6$ (Mode IX), 15a and $(\kappa^1-\kappa^0)-(\kappa^2-\kappa^0)-(\kappa^1-\kappa^0)-(\kappa^2-\kappa^0)-\mu_6$ (Mode X). 15a The H_4tptc ligands act as μ_2 - to μ_6 -linker to connect the transition metal centers, giving 1D ladder chain to 3D frameworks, which further interact with the diversity ancillary ligands, leaving the final structure varied from 1D zigzag chains to 3D high-connected frameworks.

X-ray Power Diffraction Analyses and Thermal Analyses.

In order to check the phase purity of these complexes, the PXRD patterns of title complexes were checked at room temperature. As shown in Fig. S6, the peak positions of the simulated and experimental PXRD patterns are in agreement with each other, demonstrating the good phase purity of the complexes.

Thermogravimetric analysis (TG) of complexes **1–5** was performed on samples of **1–5** under N_2 atmosphere with a heating rate of $10\text{ }^\circ\text{C min}^{-1}$, shown in Fig. 5. The TG curves for **1** and **2** show the initial weight loss below $150\text{ }^\circ\text{C}$, which can be ascribed to the removal of coordinated water molecules (observed: 4.1% and calculated: 3.5% for **1**; observed: 3.8% and calculated: 3.4% for **2**). Further weight loss observed above $350\text{ }^\circ\text{C}$ indicates the decomposition of coordination framework. For compound **3**, a gradual weight loss below $140\text{ }^\circ\text{C}$ can be attributed to the loss of

lattice water molecules (obsd. 2.1%, calc. 1.7%). Above $270\text{ }^\circ\text{C}$, the whole structure began to collapse. For compound **4**, the loss of coordinated and lattice water molecules (obsd. 6.3%, calc. 6.1%) occurred at the first weight loss below $137\text{ }^\circ\text{C}$. The second weight loss corresponding to the release of ligands is observed around $340\text{ }^\circ\text{C}$. For compound **5**, the weight loss of 4.9% from 50 to $130\text{ }^\circ\text{C}$ is attributed to the loss of coordinated and free water molecules (calc. 4.7%). The weight loss corresponding to the release of organic ligands starts at $340\text{ }^\circ\text{C}$ with a result of thermal decomposition.

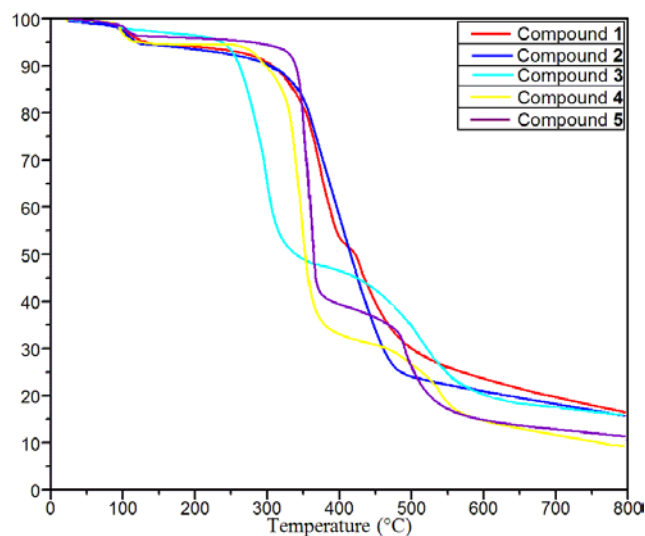


Fig. 5 TGA curves for complexes **1–5**.

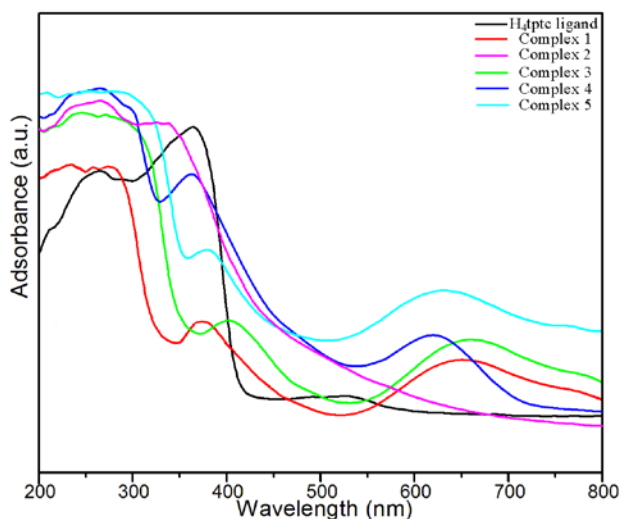


Fig. 6 UV-vis absorption spectra for H_4tptc and compounds **1-5**.

UV-Visible Absorbance Properties. The solid-state UV/vis spectra of H_4tptc and complexes **1-5** are displayed in Fig. 6. Judging from the UV/vis absorption spectra, the free ligand of H_4tptc displays absorption bands at 365 nm with a shoulder band at 264 nm due to the $\pi-\pi^*$ and $n-\pi^*$ transition of the aromatic rings.¹⁶ For Ni^{II} -based complexes, the lower energy band at 654 nm (for **1**), 657 nm (for **3**), 623 nm (for **4**), and 638 nm (for **5**) shifted from the weak band of the H_4tptc ligand at 528 nm, arising from the spin-allowed d-d transition of the d^8 (Ni^{II}) ion. The absorption band in the 200–300 nm region for complex **2** is not strongly perturbed upon its coordination to Mn^{II} , suggesting that coordination of the metal ions hardly alters the intrinsic electronic properties of H_4tptc .

Conclusions

In summary, five multi-dimensional MOFs were isolated from the hydrothermal reactions by the employment of H_4tptc and four bis(imidazole) bridging ligands (1,3-bimb, 1,4-bimb, 4,4'-bibp, and 4,4'-bimbp). Compounds **1-5** displayed appealing structural features from 2D layers to 3D frameworks, such as novel unprecedented 3D (4,4)-connected $(4^6 \cdot 8^2)_2(4^2 \cdot 8^4)$ host-framework of **3** and 2D self-catenating 5-connected $(4^6 \cdot 6^4)$ network of **4**. Structural comparison of these networks reveals that H_4tptc is an effective ligand with rich coordination modes, which is useful to better understand the synthon selectivity in multifunctional crystal structures. In addition, the employment the bis(imidazole) bridging ligands during the assemble of metal-polycarboxylate system often leads to structural changes and affords new frameworks.

Acknowledgements

The work was supported by financial support from the Natural Science Foundation of China (Grant Nos. 21101097, 91022034 and 51172127), the Excellent Youth Foundation of Shandong Scientific Committee (Grant JQ201015), Natural Science Foundation of Shandong Province (Grant ZR2010BQ023), and Qilu Normal University is acknowledged.

Notes

The authors declare no competing financial interest.

References

- (a) H. X. Deng, S. Grunder, K. E. Cordova, C. Valente, H. Furukawa, M. Hmadeh, F. Gándara, A. C. Whalley, Z. Liu, S. Asahina, H. Kazumori, M. O'Keeffe, O. Terasaki, J. F. Stoddart and O. M. Yaghi, *Nature*, 2012, **336**, 1018; (b) J. M. Lin, Y. F. Guan, D. Y. Wang, W. Dong, X. T. Wang and S. Gao, *Dalton Trans.*, 2008, 6948; (c) C. J. Li, M. X. Peng, J. D. Leng, M. M. Yang, Z. J. Lin and M. L. Tong, *CrystEngComm*, 2008, **10**, 1645; (d) X. T. Zhang, D. Sun, B. Li, L. M. Fan, B. Li and P. H. Wei, *Cryst. Growth Des.*, 2012, **12**, 3845; (e) H. C. Zhou, J. R. Long and O. M. Yaghi, *Chem. Rev.*, 2012, **112**, 673; (f) K. K. Tanabe and S. M. Cohen, *Chem. Soc. Rev.*, 2011, **40**, 498; (g) D. S. Li, Y. P. Wu, J. Zhao, J. Zhang and J. Y. Lu, *Coord. Chem. Rev.*, 2014, **261**, 1; (h) S. L. Huang, A. Q. Jia and G. X. Jin, *Chem. Commun.*, 2013, **49**, 2403; (i) S. L. Huang, L. H. Weng and G. X. Jin, *Dalton Trans.*, 2012, **41**, 11657.
- (a) M. P. Suh, H. J. Park, T. K. Prasad and D. W. Lim, *Chem. Rev.*, 2012, **112**, 782; (b) E. D. Bloch, W. L. Queen, R. Krishna, J. M. Zadrozny, C. M. Brown and J. R. Long, *Science*, 2012, **335**, 1606; (c) G. Lu, S. Li, Z. Guo, O. K. Farha, B. G. Hauser, X. Qi, Y. Wang, X. Wang, S. Han, X. Liu, J. S. Duchene, H. Zhang, Q. Zhang, X. Chen, J. Ma, S. C. Loo, W. D. Wei, Y. Yang, J. T. Hupp and F. Huo, *Nat. Chem.*, 2012, **4**, 310; (d) R. Makiura, S. Motoyama, Y. Umemura, H. Yamanaka, O. Sakata and H. Kitagawa, *Nat. Mater.*, 2010, **9**, 565; (e) S. Horike, Y. Inubushi, T. Hori, T. Fukushima and S. Kitagawa, *Chem. Sci.*, 2012, **3**, 116; (f) X. Zhang, L. Fan, Z. Sun, W. Zhang, W. Fan and X. Zhao, *CrystEngComm*, 2013, **15**, 4910; (g) X. Zhang, L. Fan, W. Zhang, Y. Ding, W. Fan and X. Zhao, *Dalton Trans.*, 2013, **42**, 16562; (h) D. S. Li, F. Fu, J. Zhao, Y. P. Wu, M. Du, K. Zou, W. W. Dong and Y. Y. Wang, *Dalton Trans.*, 2010, **39**, 11522; (i) B. Liu, D. S. Li, L. Hou, G. P. Yang, Y. Y. Wang and Q. Z. Shi, *Dalton Trans.*, 2013, **42**, 9822; (j) L. F. Ma, L. Y. Wang, J. L. Hu, Y. Y. Wang, S. R. Batten and J. G. Wang, *Dalton Trans.*, 2012, **41**, 2078.
- (a) S. V. Eliseeva and J. G. Bunzli, *Chem. Soc. Rev.*, 2010, **39**, 189; (b) B. Liu, H. B. Zheng, Z. M. Wang and S. G., *CrystEngComm*, 2011, **13**, 5285; (c) J. R. Li, R. J. Kuppler and H. C. Zhou, *Chem. Soc. Rev.*, 2009, **38**, 1477; (d) P. Coppo, M. Duati, V. N. Kozhevnikov, J. W. Hofstraat and L. D. Cola, *Angew. Chem. Int. Ed.*, 2005, **44**, 1806; (e) F. Cao, S. Wang, D. Li, S. Zeng, M. Niu, Y. Song and J. Dou, *Inorg. Chem.*, 2013, **52**, 10747; (f) J. He, M. Zeller, A. D. Hunter and Z. T. Xu, *J. Am. Chem. Soc.*, 2012, **134**, 1553; (g) Q. L. Zhang, P. Hu, Y. Zhao, G. W. Feng, Y. Q. Zhang, B. X. Zhu and Z. Tao, *J. Solid State Chem.*, 2014, **210**, 178; (h) L. F. Ma, M. L. Han, J. H. Qin, L. Y. Wang and M. Dou, *Inorg. Chem.*, 2012, **51**, 9431; (i) W. W. Dong, D. S. Li, J. Zhao, L. F. Ma, Y. P. Wu and Y. P. Duan, *CrystEngComm*, 2013, **15**, 5412; (j) D. S. Li, J. Zhao, Y. P. Wu, B. Liu, L. Bai, K. Zou and M. Du, *Inorg. Chem.*, 2013, **52**, 8091.
- (a) B. L. Chen, N. W. Ockwig, F. R. Fronczek, D. S. Contreras and O. M. Yaghi, *Inorg. Chem.*, 2005, **44**, 181; (b) S. Yang, X. Lin, A. J. Blake, K. M. Thomas, P. Hubberstey, N. R. Champness, M. Schröder, *Chem. Commun.*, 2008, **44**, 6108; (c) H. S. Choi and M. P. Suh, *Angew. Chem. Int. Ed.*, 2009, **48**, 6865; (d) B. L. Chen, N. W. Ockwig, A. R. Millward, D. S. Contreras and O. M. Yaghi, *Angew. Chem. Int. Ed.*, 2005, **44**, 4745; (e) J. L. Liu, W. Q. Lin, Y. C. Chen, J. D. Leng, F. S. Guo and M. L. Tong, *Inorg. Chem.*, 2013, **52**, 457; (f) P. H. Guo, J. L. Liu, Z. M. Zhang, L. Ungur, L. F. Chibotaru, J. D. Leng, F. S. Guo and M. L. Tong, *Inorg. Chem.*, 2012, **51**, 1233; (g) A. H. Shelton, I. V. Sazanovich, J. A. Weinstein and M. D. Ward, *Chem. Commun.*, 2012, **48**, 2749.
- (a) X. Bao, P. H. Guo, W. Liu, J. Tucek, W. X. Zhang, J. D. Leng, X. M. Chen, I. Gural'skiy, L. Salmon, A. Bousseksou and M. L. Tong, *Chem. Sci.*, 2012, **3**, 1629; (b) X. L. Zhao, D. Sun, S. Yuan, S. Y. Feng, R. Cao, D. Q. Yuan, S. N. Wang, J. M. Dou and D. F. Sun, *Inorg. Chem.*, 2012, **51**, 10350; (c) S. N. Wang, Y. Q. Peng, X. L. Wei, Q. F. Zhang, D. Q. Wang, J. M. Dou, D. C. Li and J. F. Bai,

- CrystEngComm*, 2011, **13**, 5313; (d) L. M. Fan, X. T. Zhang, D. C. Li, D. Sun, W. Zhang and J. M. Dou, *CrystEngComm*, 2013, **15**, 349; (e) C. X. Chen, Q. K. Liu, J. P. Ma and Y. B. Dong, *J. Mater. Chem.*, 2012, **22**, 9027; (f) Z. J. Lin and M. L. Tong, *Coord. Chem. Rev.*, 2011, **255**, 421; (g) T. Liu, S. Wang, J. Lu, J. Dou, M. Niu, D. Li and J. Bai, *CrystEngComm*, 2013, **15**, 5476.
6. (a) D. Sun, Y. H. Li, H. J. Hao, F. J. Liu, Y. M. Wen, R. B. Huang and L. S. Zheng, *Cryst. Growth Des.*, 2011, **11**, 3323; (b) X. J. Li, F. L. Jiang, M. Y. Wu, S. Q. Zhang, Y. F. Zhou and M. C. Hong, *Inorg. Chem.*, 2012, **51**, 4116; (c) R. Feng, L. Chen, Q. H. Chen, X. C. Shan, Y. L. Gai, F. L. Jiang and M. C. Hong, *Cryst. Growth Des.*, 2011, **11**, 1705; (d) T. M. McDonald, W. R. Lee, J. A. Mason, B. M. Wiers, C. S. Hong and J. R. Long, *J. Am. Chem. Soc.*, 2012, **134**, 7056; (e) D. S. Li, P. Zhang, J. Zhao, Z. F. Fang, M. Du, K. Zou and Y. Q. Mu, *Cryst. Growth Des.*, 2012, **12**, 1697.
7. (a) M. Suh, Y. Cheon and E. Lee, *Coord. Chem. Rev.*, 2008, **252**, 1007; (b) Y. J. Cui, Y. F. Yue, G. D. Qian and B. L. Chen, *Chem. Rev.*, 2012, **112**, 1126; (c) B. Lebeau and P. Innocenzi, *Chem. Soc. Rev.*, 2011, **40**, 886; (d) S. T. Meek, J. A. Greathouse and M. D. Allendorf, *Adv. Mater.*, 2011, **23**, 249; (e) C. G. Silva, A. Corma and H. Garcia, *J. Mater. Chem.*, 2010, **20**, 3141.
8. (a) A. Thirumurugan and S. Natarajan, *J. Mater. Chem.*, 2005, **15**, 4588; (b) D. C. Zhong, J. H. Deng, X. Z. Luo, H. J. Liu, J. L. Zhong, K. J. Wang and T. B. Lu, *Cryst. Growth Des.*, 2012, **12**, 1992; (c) L. B. Sun, Y. Li, Z. Q. Liang, J. H. Yu and R. R. Xu, *Dalton Trans.*, 2012, **41**, 12790; (d) G. Liu and H. Li, *CrystEngComm*, 2013, **15**, 6870; (e) J. J. Wang, T. T. Wang, L. Tang, X. Y. Hou, L. J. Gao, F. Fu and M. L. Zhang, *J. Coord. Chem.*, 2013, **66**, 3979.
9. (a) X. Lin, I. Telepeni, A. J. Blake, A. Dailly, C. M. Brown, J. M. Simmons, M. Zoppi, G. S. Walker, K. M. Thomas, T. J. Mays, P. Hubberstey, N. R. Champness and M. Schröder, *J. Am. Chem. Soc.*, 2009, **131**, 2159; (b) S. Q. Ma, J. P. Simmons, D. F. Sun, D. Q. Yuan and H. C. Zhou, *Inorg. Chem.*, 2009, **48**, 5263; (c) X. Lin, J.-H. Jia, X.-B. Zhao, K. M. Thomas, A. J. Blake, G. S. Walker, N. R. Champness, P. Hubberstey and M. Schröder, *Angew. Chem. Int. Ed.*, 2006, **45**, 7358.
10. (a) F. Guo, F. Wang, H. Yang, X. L. Zhang and J. Zhang, *Inorg. Chem.*, 2012, **51**, 9677; (b) L. Fan, X. Zhang, Z. Sun, W. Zhang, Y. Ding, W. Fan, L. Sun, X. Zhao and H. Lei, *Cryst. Growth Des.*, 2013, **13**, 2462; (c) X. Zhang, L. Fan, Z. Sun, W. Zhang, D. Li, J. Dou and L. Han, *Cryst. Growth Des.*, 2013, **13**, 792; (d) T. Wu, Y. J. Lin and G. X. Jin, *Dalton Trans.*, 2013, **42**, 82; (e) L. Fan, X. Zhang, W. Zhang, Y. Ding, L. Sun, W. Fan and X. Zhao, *CrystEngComm*, 2013, DOI: 10.1039/C3CE42203H.
11. (a) G. M. Sheldrick, *SHELXTL*, version 5.1; Bruker Analytical X-ray Instruments Inc.: Madison, WI, 1998. (b) G. M. Sheldrick, *SHELX-97*, PC Version; University of Gottingen: Gottingen, Germany, 1997.
12. (a) G. Mehlana, S. A. Bourne, G. Ramon and L. Ohrstrom, *Cryst. Growth Des.*, 2013, **13**, 633; (b) D. Martini, M. Pellei, C. Pettinari, B. W. Skelton and A. H. White, *Inorg. Chim. Acta*, 2002, **333**, 72.
13. (a) A. L. Spek, *J. Appl. Crystallogr.*, 2003, **36**, 7; (b) A. L. Spek, *PLATON, A Multipurpose Crystallographic Tool*, Utrecht University, Utrecht, The Netherlands, 2002.
14. (a) V. A. Blatov, A. P. Shevchenko and V. N. Serezhkin, *J. Appl. Crystallogr.*, 2000, **33**, 1193; (b) The network topology was evaluated by the program "TOPOS-4.0", see: <http://www.topos.ssu.samara.ru>. (c) V. A. Blatov, M. O'Keeffe and D. M. Proserpio, *CrystEngComm*, 2010, **12**, 44.
15. (a) X. T. Zhang, L. M. Fan, X. Zhao, D. Sun, D. C. Li and J. M. Dou, *CrystEngComm*, 2012, **14**, 2053; (b) X. Zhang, L. Fan, Z. Sun, W. Zhang, D. Li, P. Wei, B. Li and J. Dou, *J. Coord. Chem.*, 2012, **65**, 3205; (c) L. Fan, X. Zhang, Z. Sun, W. Zhang, D. Li, P. Wei, B. Li and J. Dou, *J. Coord. Chem.*, 2012, **65**, 4389; (d) X. T. Zhang, L. M. Fan, Z. Sun, W. Zhang, D. C. Li, P. H. Wei, B. Li, G. Z. Liu and J. M. Dou, *Chinese J. Inorg. Chem.*, 2012, **28**, 1809; (e) X. T. Zhang, L. Q. Zhang, L. D. Zhang, L. M. Fan, P. H. Wei and S. X. Zhang, *Chinese J. Struct. Chem.*, 2012, **31**, 1518; (f) W. Zhang and H. Y. Zhu, *Chinese J. Struct. Chem.*, 2012, **31**, 1701.
16. (a) M. M. Dong, L. L. He, Y. J. Fan, S. Q. Zang, H. W. Hou and T. C. W. Mak, *Cryst. Growth Des.*, 2013, **13**, 3353; (b) Z. Q. Shi, Y. Z. Li, Z. J. Guo and H. G. Zheng, *Cryst. Growth Des.*, 2013, **13**, 3078; (c) C. R. K. Glasson, G. V. Meehan, C. A. Motti, J. K. Clegg, P. Truner, P. Jensen and L. F. Lindoy, *Dalton Trans.*, 2011, **40**, 10481; (d) S. Pandey, P. P. Das, A. K. Singh and R. Mukherjee, *Dalton Trans.*, 2011, **40**, 10758.

Table of Contents Graphic and Synopsis

Syntheses, Crystal Structures, UV-Visible Absorption Properties of Five Coordination Polymers Based on Terphenyl-2,5,2',5'-tetracarboxylic Acid and Bis(imidazole) Bridging Ligands

5 Liming Fan, Xiutang Zhang, Wei Zhang, Yuanshuai Ding, Weiliu Fan, Liming Sun, Yue Pang, Xian Zhao

Five novel coordination polymers based on terphenyl-2,5,2',5'-tetracarboxylic acid and bis(imidazole) bridging ligands. Complexes **1** and **2** exhibit 3D (3,4)-connected **tfi** frameworks with the Point Schläfli symbol of $(4\cdot 6^2)(4\cdot 6^6\cdot 8^3)$. Complex **3** shows an unprecedented 3D (4,4)-connected frameworks with the Point Schläfli symbol of $(4\cdot 6^4\cdot 8^2)_2(4^2\cdot 8^4)$. Complex **4** displays a novel 2D self-catenating 5-connected network with the Schläfli symbol of $(4^6\cdot 6^4)$ based on three interpenetrating 4^4 -**sql** subnets. Complex **5** features a 2D 3-connected 6^3 -**hcb** networks based on the interestingly chain with loops.

